Weierstraß-Institut
für Angewandte Analysis und Stochastik
Leibniz-Institut im Forschungsverbund Berlin e. V.

Preprint ISSN 2198-5855

Robust equilibration a posteriori error estimation for convection-diffusion-reaction problems

new title: **Equilibration a posteriori error estimation for convection-diffusion-reaction problems**

Martin Eigel[1], Christian Merdon[2]

submitted: June 30, 2013

updated: December 22, 2014

[1] Weierstrass Institute
Mohrenstr. 39
10117 Berlin
Germany
E-Mail: martin.eigel@wias-berlin.de

[2] Humboldt-Universität zu Berlin
Department of Mathematics
Unter den Linden 6
10099 Berlin
Germany
E-Mail: merdon@mathematik.hu-berlin.de

No. 1822
Berlin 2013

2010 *Mathematics Subject Classification.* 65N30, 65N15, 65J15, 65N22, 65J10.

Key words and phrases. A posteriori, error analysis, finite element method, equilibrated, convection dominated, adaptivity, inhomogeneous Dirichlet, augmented norm.

Edited by
Weierstraß-Institut für Angewandte Analysis und Stochastik (WIAS)
Leibniz-Institut im Forschungsverbund Berlin e. V.
Mohrenstraße 39
10117 Berlin
Germany

Fax: +49 30 20372-303
E-Mail: preprint@wias-berlin.de
World Wide Web: http://www.wias-berlin.de/

ZUSAMMENFASSUNG. We study a posteriori error estimates for convection-diffusion-reaction problems with possibly dominating convection or reaction and inhomogeneous boundary conditions. For the conforming FEM discretisation with streamline diffusion stabilisation (SDM), we derive reliable and efficient error estimators based on the reconstruction of equilibrated fluxes in an admissible discrete subspace of $H(\operatorname{div}, \Omega)$. Error estimators of this type have become popular recently since they provide guaranteed error bounds without further unknown constants. The estimators can be improved significantly by some postprocessing and divergence correction technique. For an extension of the energy norm by a dual norm of the convection part of the differential operator, robustness of the error estimator with respect to the coefficients of the problem is achieved.

Numerical benchmarks illustrate the good performance of the error estimators for singularly perturbed problems, in particular with dominating convection.

1. INTRODUCTION

On some polygonal domain $\Omega \subset \mathbb{R}^d$ ($d = 2, 3$) we consider the stationary convection-diffusion-reaction problem

$$-\nabla \cdot (K\nabla u) + \beta \cdot \nabla u + \mu u = f \qquad \text{in } \Omega, \tag{1.1}$$

$$u = u_D \quad \text{on } \Gamma_D \qquad \text{and} \qquad K\frac{\partial u}{\partial n} = g \quad \text{on } \Gamma_N. \tag{1.2}$$

The Lipschitz boundary $\partial\Omega$ consists of a closed Dirichlet boundary Γ_D with non-zero surface measure and data u_D, and a Neumann boundary $\Gamma_N = \partial\Omega \setminus \Gamma_D$ with data g. K denotes the diffusion tensor, β some velocity field, μ the reaction coefficient and f the source term. The exact prerequisites of the data are given in detail in Section 2.

We consider a posteriori error estimators for the error $e := u - u_h$ of some conforming first-order stabilised FEM approximation u_h measured in the energy norm. This notion of a posteriori error control in the energy norm induced by the operator in computational PDE has been a vivid area of research for a long time. It has become increasingly evident that the crucial task is the evaluation of computational bounds for the dual norm of some appropriate (problem dependent) residual $\mathcal{R}es \in H^{-1}(\Omega)$ in the dual space of the standard first-order Sobolev space with homogeneous boundary values. This in particular was elucidated by the unified approach of Carstensen, see e.g. [CEHL12].

A posteriori error control reached a substantial maturity with the advent of efficient and generic evaluation techniques for equilibrated flux reconstruction [DM99, LW04, BS08] and the error majorants by Repin [RS06, Rep08]. A crucial benefit of these type of estimators is that they allow for guaranteed error bounds without unknown constants. This remedies a major shortcoming which has plagued a posteriori error control before. While equilibrated flux estimators have been systematically analysed and compared for several standard second order model problems [CM10, CM13], there are only very few contributions [CFPV09, AABR13] for the problem at hand.

In [ESV10], an error estimator similar to the one derived in this work is presented. The main difference is the choice of the discretisation (discontinuous Galerkin as opposed to conforming first-order FEM) and the resulting implications for the equilibration terms. By using a more classical stabilised discretisation (which in particular is commonly used in engineering applications), in our opinion the presentation of the error estimator in this paper appears clearer and less cluttered with technical notation. We address some of the most accurate energy norm error estimators which can be written as equilibrium error estimators. These are based on the design of some $q \in H(\operatorname{div}, \Omega)$ which satisfies

$$\operatorname{div} q + \widehat{f} = 0 \text{ in } \Omega \quad \text{and} \quad q \cdot \nu - g = 0 \text{ along } \Gamma_N$$

with some modified right-hand side $\widehat{f} \in L^2(\Omega)$. It turns out that additional terms that arise from the SDM stabilisation can be controlled properly. Moreover, we provide a thorough comparison of different flux designs for a set of benchmark problems to illustrate their performance. We also demonstrate recent flux optimisation techniques, namely some postprocessing on refined grids and some divergence correction which in certain situations can improve the evaluated upper error bound significantly.

Classical error estimators for problem (1.1) were e.g. examined in [Ver05, Ver98] and numerical assessments were provided in [PV00] and [Joh00]. In [Ver05], Verfürth introduced the notion of an extension of the energy norm by some dual norm related to the convective part of the operator. This idea, which renders the error estimator significantly more efficient and fully stable with respect to the coefficients of the problem even in the convection or reaction dominated case, is also key in the derivations suggested in [ESV10] and [AABR13]. We adopt this notion of the so-called augmented norm for some numerical examples and illustrate the effect this modified norm has on the efficiency of the error estimator.

Some of the numerical examples of Section 5 are chosen identically to these references to allow for a comparison of different error estimators.

Here and throughout the paper, we employ the standard notation for Lebesgue and Sobolev spaces and their norms. In particular, $H^1_D(\Omega) := \{v \in H^1(\Omega) \mid v|_{\Gamma_D} = 0\}$.

In Section 2, some further notation and assumptions on the coefficients are set. Moreover, the finite element method and the streamline diffusion stabilisation for convection dominated problems is introduced. By this, the related modified residual $\mathcal{R}es_{\mathrm{SDM}}$ is defined. Section 3 contains the main results of this work and is dedicated to the derivation of several equilibration error estimators. Some specific constructions of numerical fluxes and possible improvements are described. Moreover, the treatment of inhomogeneous Dirichlet boundary data is examined. Section 4 deals with the efficiency of the error estimators with focus on the convection-dominated case. Numerical experiments in Section 5 illustrate the performance of the derived a posteriori error estimators based on a set of benchmark problems.

2. Setting

2.1. **Notation and assumptions.** We assume a piecewise domain $\Omega \subset \mathbb{R}^d$ ($d = 2, 3$) and its regular partition $\mathcal{T}$ into triangles (for $d = 2$) or tetrahedra (for $d = 3$) $T \in \mathcal{T}$ with faces $E \in \mathcal{E}$ and the set of vertices $\mathcal{N}$, see [Cia78]. Any two elements of $\mathcal{T}$ share at most one common face (or two vertices in 3D) or one vertex and all elements are shape regular, i.e., the ratio of the smallest circumscribed ball and the largest ball inscribed is bounded by a constant which does not depend on the cell for any $T \in \mathcal{T}$. The local mesh-size function reads $h := h_T := \mathrm{diam}(T)$ on $T \in \mathcal{T}$. The jump of $v \in L^2(\Omega)$ along some face $E \in \mathcal{E}$ is denoted by $[v]_E$ and the outer unit normal vector with regard to E is denoted by ν_E. The patch of some node $z \in \mathcal{N}$ or a face $E \in \mathcal{E}$ is defined by $\omega_z := \mathcal{T}(z) := \{T \in \mathcal{T} \mid z \in T\}$ or $\omega_E := \mathcal{T}(E) := \{T \in \mathcal{T} \mid E \in T\}$, respectively. We further define the subsets $\mathcal{E}(z) := \{E \in \mathcal{E} \mid z \in E\}$ and $\mathcal{N}(T) := \{z \in \mathcal{N} \mid z \in T\}$. By $\mathcal{E}(\Gamma_N) := \mathcal{E}_N := \{E \in \mathcal{E} \mid |E \cap \Gamma_N| > 0\}$ and $\mathcal{N}(\Gamma_D) := \{z \in \mathcal{N} \mid z \in \Gamma_D\}$ we denote the set of faces which lie on the Neumann boundary and the set of nodes on the Dirichlet boundary. In 2D, the red-refinement $\mathrm{red}(T)$ of a triangle $T \in \mathcal{T}$ results in a partition into four sub-triangles by connecting the face mid-points $\mathrm{mid}(\mathcal{E}(T))$ by three new faces. A complete red-refinement $\mathrm{red}(\mathcal{T})$ results from the red-refinement of all elements $T \in \mathcal{T}$. Moreover, define the (conforming) discrete space

$$V_h := \big\{v \in C(\overline{\Omega}) \mid \forall T \in \mathcal{T}\ v|_T \in P_1(T) \text{ and } v = 0 \text{ on } \Gamma_D\big\} \subset V := H^1_D(\Omega)$$

where P_1 is the space of polynomials of maximal degree one. We denote by $\varphi_z \in V_h$ the nodal affine basis function associated with node $z \in \mathcal{N}_h$ with support ω_z, $\varphi_z(z) = 1$ and $\varphi(z') = 0$ for all $z' \in \mathcal{N}_h \setminus \{z\}$.

The discrete Raviart-Thomas spaces of order k are defined on $T \in \mathcal{T}_h$ by

$$\mathrm{RT}_k(T) := \big\{v \in P_{k+1}(T, \mathbb{R}^d) \mid \exists\, a_0, \dots, a_d \in P_k(T) \text{ s.t. } \forall x \in T,$$
$$v(x) = (a_1, \dots, a_d) + a_0 x\big\}$$

while the broken Raviart-Thomas space of order 0 is defined by

$$\mathrm{RT}_{-1}(\mathcal{T}_h) := \big\{v \in L^2\left(\Omega, \mathbb{R}^d\right) \mid \forall T \in \mathcal{T}_h\ v|_T \in \mathrm{RT}_0(T)\big\}.$$

For the data in (1.1) we assume that $K \in L^\infty(\Omega)^{d\times d}$ is a symmetric positive definite and piecewise constant tensor. Moreover, we assume that $\beta \in H(\mathrm{div}, \Omega) \cap L^\infty(\Omega)$, $\mu \in L^\infty(\Omega)$ and $\mu - \frac{1}{2}\,\mathrm{div}\,\beta \geq 0$ a.e. in Ω. By $c_{K,T}$ we denote the smallest eigenvalue of K and by $c_{\beta,\mu,T}$ the smallest value of $\mu - \frac{1}{2}\,\mathrm{div}\,\beta$ on $T \in \mathcal{T}_h$. In case that $c_{\beta,\mu,T} = 0$, we suppose that $\|\mu\|_{L^\infty(T)} = \left\|\frac{1}{2}\,\mathrm{div}\,\beta\right\|_{L^\infty(T)} = 0$. Additionally, the boundary data u_D and g are assumed to be sufficiently smooth where the Dirichlet data is approximated by $u_{\mathrm{D,h}} := \sum_{z\in\mathcal{N}(\Gamma_D)} u_D(z)\varphi_z$.

2.2. **The continuous problem.** We define the bilinear form according to problem (1.1)

$$a(u, v) := \int_\Omega K\nabla u \cdot \nabla v\, dx + \int_\Omega (\beta \cdot \nabla u + \mu u)v\, dx.$$

The induced energy (semi)norm $\|\!|v|\!\|^2 := a(v,v)$ can be written as

$$\|\!|v|\!\|^2 := \sum_{T\in\mathcal{T}_h} \|\!|v|\!\|_T^2 \text{ with } \|\!|v|\!\|_T^2 := \left\|K^{1/2}\nabla v\right\|_T^2 + \left\|\left(\mu - \frac{1}{2}\operatorname{div}\beta\right)^{1/2} v\right\|_T^2$$

and the weak formulation is given by: Find $u \in u_{\mathrm{D,h}} + V$ such that

$$a(u,v) = \int_\Omega fv\, dx + \int_{\Gamma_N} gv\, ds \quad \text{for all } v \in V. \tag{2.1}$$

For the later analysis similar to [ESV10], we split the bilinear form $a = a_S + a_A$ with

$$a_S(u,v) := \int_\Omega K\nabla u \cdot \nabla v\, dx + \int_\Omega \left(\mu - \frac{1}{2}\operatorname{div}\beta\right) uv\, dx \quad \text{and} \tag{2.2}$$

$$a_A(u,v) := \int_\Omega \left(\beta\cdot\nabla u + \frac{1}{2}\operatorname{div}\beta u\right) v\, dx. \tag{2.3}$$

2.3. **The discrete problem.** The standard FEM discretisation of the weak formulation (2.1) reads: Find $u_h \in u_{\mathrm{D,h}} + V_h$ such that

$$a(u_h,v) = \int_\Omega fv\, dx + \int_{\Gamma_N} gv\, ds \quad \text{for all } v \in V_h. \tag{2.4}$$

For the common case of dominant convection, the standard finite element method is not a stable discretisation. This can be observed by the appearance of spurious oscillations in the solution. To circumvent this unphysical behaviour, the stability of the discretisation is increased by the addition of some artificial diffusion to the standard weak form of the problem. For this, as a simple and frequently employed stabilisation technique, we recall the streamline diffusion method (SDM) which exhibits good stability properties and high-order accuracy. We refer to [EJ93, Joh90, JNP84] for details on the SDM which is also called streamline-upwind Petrov-Galerkin method (SUPG) as in the references [HB79, HMM86].

Instead of a test function v as in (2.4), we now use $w = v + \delta\beta\cdot\nabla v$. The additional term accounts for the vector field β. Several choices for the scaling δ are discussed in the literature. Usually, it is expressed as a function of the local Péclet number $\mathrm{Pe}^h := 1/2\,|\beta|\, h_T/c_{K,T}$ which depends on the local mesh size h_T, and the problem coefficients K and β, with

$$\delta_T := \frac{h_T}{2\,|\beta|}\zeta(\mathrm{Pe}^h) \qquad \text{for any } T \in \mathcal{T}.$$

For our computations, we employ $\zeta(\mathrm{Pe}^h) := \max\{0, 1 - 1/(2\mathrm{Pe}^h)\}$ from [PV00], also see [EJ93].

With the SDM discretisation, the modified bilinear and linear forms for the system (2.4) are defined by

$$a_{\mathrm{SDM}}(u_h,v) := a(u_h,v) + \sum_{T\in\mathcal{T}}\int_T \left(-\operatorname{div}(K\nabla u_h) + \beta\cdot\nabla u_h + \mu u_h\right)\delta\beta\cdot\nabla v\, dx, \tag{2.5}$$

$$\ell_{\mathrm{SDM}}(v) := \int_\Omega f(v + \delta\beta\cdot\nabla v)\, dx + \int_{\Gamma_N} gv\, ds. \tag{2.6}$$

The stabilised variational problem reads: Find $u_h \in u_{\mathrm{D,h}} + V_h$ such that

$$a_{\mathrm{SDM}}(u_h,v_h) = \ell_{\mathrm{SDM}}(v_h) \qquad \text{for all } v_h \in V_h. \tag{2.7}$$

3. Equilibrated Error Estimators

3.1. **Residual and error identity.** According to (2.1), we define the residual, for any $v \in V$ and $\sigma_h := K\nabla u_h$,

$$\mathcal{R}es(v) := a(u - u_h, v) = \int_\Omega \widehat{f} v\, dx + \int_{\Gamma_N} gv\, ds - \int_\Omega \sigma_h\cdot\nabla v\, dx \tag{3.1}$$

with $\widehat{f} := f - \beta\cdot\nabla u_h - \mu u_h$.

It is well-known [BC04] that for homogeneous Dirichlet data the dual norm of the residual

$$\|\mathcal{R}es\|_* := \sup_{\substack{v\in V\\ \|v\|=1}} \mathcal{R}es(v)$$

is an upper bound of the energy norm of the error, see Theorem 3.2 below for $u_D = 0$. In case of inhomogeneous Dirichlet data, $v = u - u_h$ is not a valid test function but it still holds an inequality of the form

$$\|u - u_h\|^2 \leq \|\mathcal{R}es\|_*^2 + \|w_D\|^2 .$$

The term $\|w_D\|$ on the right-hand side is discussed in Subsection 3.3.

For the stabilised problem (2.7), we define the auxiliary residual

$$\mathcal{R}es_{\text{SDM}}(v) := \ell_{\text{SDM}}(v) - a_{\text{SDM}}(u_h, v) = \mathcal{R}es(v) + G(v) \tag{3.2}$$

where

$$G(v) := \delta\left(\int_\Omega \widehat{f}\beta\cdot\nabla v\ dx\right).$$

Note that for $u \in H^2(\mathcal{T})$, $\mathcal{R}es_{\text{SDM}}(v) = a_{\text{SDM}}(u - u_h, v)$ is satisfied.

3.2. **Equilibration.** For any free node $z \in \mathcal{N}$, (2.7) shows

$$\mathcal{R}es_{\text{SDM}}(\varphi_z) = \int_\Omega \widehat{f}\varphi_z\ dx + \int_{\Gamma_N} g\varphi_z\ ds - \int_\Omega \sigma_h\cdot\nabla\varphi_z\ dx + G(\varphi_z) = 0.$$

This allows for the local design of equilibrated fluxes $q \in H(\text{div}, \Omega)$ in the ansatz

$$\begin{aligned}\mathcal{R}es_{\text{SDM}}(v) = &\int_\Omega (\widehat{f} + \operatorname{div} q)v\ dx + \int_{\Gamma_N} (g - q\cdot\nu)v\ ds\\ &+ \int_\Omega (q - \sigma_h)\cdot\nabla v\ dx + G(v).\end{aligned} \tag{3.3}$$

Three designs for appropriate numerical fluxes q after [DM99, BS08, LW04, CM12a] are given below. They are equilibrated in the sense that

$$\operatorname{div} q + \widehat{f}_h = 0 \text{ in } \Omega \quad\text{and}\quad q\cdot\nu - g_h = 0 \text{ along } \Gamma_N. \tag{3.4}$$

Here, $\widehat{f}_h$ is some approximation of the extended source term $\widehat{f}$ such that $\int_T \widehat{f} - \widehat{f}_h\ dx = 0$ for $T \in \mathcal{T}$ and g_h approximates g such that $\int_E g - g_h\ dx = 0$ for $E \in \mathcal{E}_N$. The approaches of Destuynder-Métivet or Braess and Luce-Wohlmuth lead to different approximations $\widehat{f}_h$ and g_h. However, the analysis for all designs leads to the locally computable error estimator contributions on $T \in \mathcal{T}$,

$$\eta_{R,T}(q) := m_T \left\|\widehat{f} - \widehat{f}_h\right\|_T + \sum_{E\in\mathcal{E}_N\cap\mathcal{E}(T)} m_{E,N}\,\|g - g_h\|_E , \tag{3.5}$$

$$\eta_{\text{DF},T}(q) := \left\|K^{-1/2}(q - \sigma_h)\right\|_T , \tag{3.6}$$

with the explicit constants $m_T^2 := \min\{C_P^2 h_T^2 c_{K,T}^{-1}, c_{\beta,\mu,T}^{-1}\}$ and $m_{E,N}^2 := |E|\,/\,|T|\,(m_T^2 + h_T {c_{K,T}}^{-1/2} m_T)$ where C_P denotes the Poincaré constant. On triangles in 2D, $C_P = 1/j_{1,1}$ where $j_{1,1}$ is the first positive root of the first Bessel function J_1, see [LS10]. In 3D, there is the Payne-Weinberger constant $C_P = 1/\pi$ for convex domains, see [PW60, Beb03].

Theorem 3.1. *For any $q \in H(\text{div}, \Omega)$ that satisfies* (3.4) *with $\int_T \widehat{f} - \widehat{f}_h\ dx = 0$ for all $T \in \mathcal{T}$ as well as $\int_E g - g_h\ dx = 0$ for all $E \in \mathcal{E}_N$, it holds*

$$\|\mathcal{R}es\|_* \leq \left(\sum_{T\in\mathcal{T}} (\eta_{R,T}(q) + \eta_{DF,T}(q))^2\right)^{1/2} . \tag{3.7}$$

Beweis. It holds, for any $v \in V$,

$$\begin{aligned}\mathcal{R}es(v) &= \int_\Omega (\widehat{f} + \operatorname{div} q) v \, dx + \int_{\Gamma_N} (g - q\cdot\nu) v \, ds + \int_\Omega (q-\sigma_h)\cdot\nabla v \, dx \\ &= \int_\Omega (\widehat{f} - \widehat{f}_h)(v - v_{\mathcal{T}}) \, dx + \int_{\Gamma_N} (g - g_h) v \, ds \\ &\quad + \int_\Omega K^{-1/2}(q-\sigma_h)\cdot K^{1/2}\nabla v \, dx.\end{aligned}$$

The arbitrary constant v_T is set to $v_T := \int_T v \, dx / |T|$ or $v_T = 0$ (whichever leads to the better estimate) and $v_{\mathcal{T}}|_T = v_T$ for all $T \in \mathcal{T}$. Then, elementwise Cauchy and Poincaré inequalities on every $T \in \mathcal{T}$ show

$$\int_\Omega (\widehat{f} - \widehat{f}_h)(v - v_{\mathcal{T}}) \, dx \leq \sum_{T\in\mathcal{T}} m_T \left\| \widehat{f} - \widehat{f}_h \right\|_T \|\!|v|\!\|_T .$$

For g_h with $\int_E (g - g_h) \, ds = 0$ on all Neumann boundary faces $E \in \mathcal{E}_N$, it follows, for any constant v_E,

$$\int_E (g-g_h) v \, ds = \int_E (g-g_h)(v - v_E) \, ds \leq \|g - g_h\|_{L^2(E)} \|v - v_E\|_{L^2(E)} .$$

A trace identity for E and a neighbouring element $T = \operatorname{conv}\{E, P\} \in \mathcal{T}$ with a vertex P opposite to E shows

$$\|v - v_E\|^2_{L^2(E)} = \frac{|E|}{|T|}\int_T (v-v_E)^2 \, dx + \frac{|E|}{2\,|T|}\int_T (x-P)\cdot\nabla((v-v_E)^2) \, dx.$$

Elementary calculations with $\nabla((v-v_E)^2) = 2(v-v_E)\nabla(v)$, $|x - P| \leq h_T$ and Poincaré inequalities for the choice $v_E := \int_T v \, dx/|T|$ (or $v_E = 0$ without further estimation) lead to

$$\begin{aligned}\|v - v_E\|^2_{L^2(E)} &\leq \frac{|E|}{|T|}\left(m_T^2 \|\!|v|\!\|_T^2 + h_T \|v - v_E\|_{L^2(T)} \|\nabla v\|_{L^2(T)} \right) \\ &\leq \frac{|E|}{|T|}\left(m_T^2 + h_T {c_{K,T}}^{-1/2} m_T \right) \|\!|v|\!\|_T^2 = m_{E,N}^2 \|\!|v|\!\|_T^2 .\end{aligned}$$

The combination of the previous results and a Cauchy inequality in $\mathbb{R}^{|\mathcal{T}|}$ yield

$$\mathcal{R}es(v) \leq \sum_{T\in\mathcal{T}} (\eta_{R,T}(q) + \eta_{\mathrm{DF},T}(q)) \|\!|v|\!\|_T \qquad \leq \left(\sum_{T\in\mathcal{T}} (\eta_{R,T}(q) + \eta_{\mathrm{DF},T}(q))^2 \right)^{1/2} \|\!|v|\!\| .$$

A division by $\|\!|v|\!\|$ concludes the proof. □

Particular designs of q were e.g. suggested by Destuynder, Métivet [DM99], Braess [BS08], Luce and Wohlmuth [LW04] and Vohralik [Voh07]. We provide the details of two designs and slight modifications due to the presence of the stabilisation as in [AABR13]. Subsection 3.2.3 describes an alternative global minimisation based on the Raviart-Thomas mixed FEM.

3.2.1. *Equilibration after Destuynder, Métivet and Braess.* The design inspired by Destuynder, Métivet [DM99] and Braess [BS08] solves local problems on node patches. For every $z \in \mathcal{N}$, the design involves the piecewise constant function $\widehat{f}_z \in P_0(\mathcal{T}(z))$ and $g_z \in P_0(\mathcal{E}(z) \cap \mathcal{E}_N)$ defined by

$$\begin{aligned}\widehat{f}_z|_T &:= |T|^{-1}\left(\int_T \widehat{f}\varphi_z \, dx + \delta_T \int_T \widehat{f}\beta\cdot\nabla\varphi_z \, dx \right) \quad \text{for } T \in \mathcal{T}(z), \\ g_z|_E &:= |E|^{-1}\left(\int_E g\varphi_z \, ds \right) \quad \text{for } E \in \mathcal{E}(z)\cap\mathcal{E}_N.\end{aligned}$$

Then, $q_z \in \mathrm{RT}_{-1}(\mathcal{T}(z))$ is the solution of the local minimisation problem

$$\begin{aligned}q_z = \operatorname*{argmin}_{\tau_z \in \mathrm{RT}_{-1}(\mathcal{T}(z))} \Big\{ \left\| K^{-1/2}\tau_z \right\|_{L^2(\omega_z)} \mid \operatorname{div}\tau_z + \widehat{f}_z = 0, \tau_z\cdot\nu = 0 \text{ along } \partial\omega_z \setminus \partial\Omega, \\ \tau_z\cdot\nu = g_z - \frac{1}{d}\sigma_h\cdot\nu \text{ along } \partial\omega_z\cap\Gamma_N, \text{ and } [\tau_z\cdot\nu] = -\frac{1}{d}[\sigma_h\cdot\nu] \text{ for all } E \in \mathcal{E}(z)\setminus\mathcal{E}_N \Big\}.\end{aligned}$$

The existence of q_z for $z \in \mathcal{N} \setminus \mathcal{N}(\Gamma_D)$ follows from $\mathcal{R}es_{\mathrm{SDM}}(\varphi_z) = 0$ and the complementary condition

$$\begin{aligned}
\int_{\omega_z} \operatorname{div} q_z \, dx &= \sum_{E \in \mathcal{E}(z) \setminus \mathcal{E}_N} \int_E [q_z \cdot \nu] \, ds + \int_{\Gamma_N \cap \partial\omega_z} q_z \cdot \nu \, ds \\
&= \sum_{E \in \mathcal{E}(z) \setminus \mathcal{E}_N} \int_E \varphi_z [\sigma_h \cdot \nu] \, ds + \int_{\Gamma_N \cap \partial\omega_z} q_z \cdot \nu \, ds \\
&= -\int_{\omega_z} \sigma_h \cdot \nabla \varphi_z \, dx + \int_{\Gamma_N \cap \partial\omega_z} (q_z + \sigma_h) \cdot \nu \, ds \\
&= \mathcal{R}es_{\mathrm{SDM}}(\varphi_z) - \int_{\omega_z} \widehat{f} \varphi_z \, dx - G(\varphi_z) \\
&\quad + \int_{\Gamma_N \cap \partial\omega_z} (q_z + \varphi_z \sigma_h) \cdot \nu - g\varphi_z \, ds \\
&= -\int_{\omega_z} \widehat{f} \varphi_z \, dx - G(\varphi_z) + \int_{\Gamma_N \cap \partial\omega_z} (q_z + 1/d \, \sigma_h) \cdot \nu - g\varphi_z \, ds.
\end{aligned}$$

Hence, q_z must satisfy

$$\int_{\omega_z} \operatorname{div} q_z + \widehat{f} \varphi_z \, dx + \int_{\Gamma_N \cap \partial\omega_z} (g\varphi_z - 1/d \, \sigma_h \cdot \nu) - q_z \cdot \nu \, ds + G(\varphi_z) = 0$$

which is ensured with the constraints above. This condition can be found also in [AABR13, formula (32)]. The sum of all local solutions leads to $q_{\mathrm{B}} := \sigma_h + \sum_{z \in \mathcal{N}} q_z \in \mathrm{RT}_0(\mathcal{T})$ with $q_z \cdot \nu = g_E = \int_E g \, ds / |E|$ for all $E \in \mathcal{E}_N$ and

$$-\operatorname{div} q_{\mathrm{B}}|_T = \sum_{z \in \mathcal{N}(T)} \operatorname{div} q_z = \widehat{f}_T = \int_T \widehat{f} \, dx / |T| \quad \text{for all } T \in \mathcal{T}.$$

Note that the local contributions of $\int_T \widehat{f} \beta \cdot \nabla \varphi_z \, dx$ in q_{B} sum up to

$$\sum_{z \in \mathcal{N}(T)} \int_T \widehat{f} \beta \cdot \nabla \varphi_z \, dx = \int_T \widehat{f} \beta \cdot \nabla \sum_{z \in \mathcal{N}(T)} \varphi_z \, dx = 0.$$

Theorem 3.1 with $\widehat{f}_h = \widehat{f}_{\mathcal{T}}$ for the piecewise integral mean of $\widehat{f}$, and $g_h = g_{\mathcal{E}_N}$ for the facewise integral mean of g, yields

$$|||\mathcal{R}es|||_* \leq \left(\sum_{T \in \mathcal{T}} \left(\eta_{R,T}(q_{\mathrm{B}}) + \eta_{\mathrm{DF},T}(q_{\mathrm{B}}) \right)^2 \right)^{1/2} =: \eta_B.$$

3.2.2. *Equilibration after Luce and Wohlmuth.* The Luce-Wohlmuth design after [LW04] employs the dual triangulation $\mathcal{T}^\star$. It connects the element centers $\mathrm{mid}(T)$ with adjacent nodes and face midpoints (and also edge midpoints in 3D) and so divides every element $T \in \mathcal{T}$ into $(d+1)!$ subelements of equal area $|T|/(d+1)!$. The nodal basis functions of nodes $z \in \mathcal{N}^*$ in the dual mesh are denoted by φ_z^* and their patch is denoted by ω_z^*.

The further design employs an interpolation $f^\star \in P_0(\mathcal{T}^\star)$ of f and $g^\star \in P_0(\mathcal{E}^\star)$ from [CM12b] defined by

$$f^\star|_{T \cap \omega_z^\star} := (d+1) \int_T \widehat{f} \varphi_z \, dx / |T| \quad \text{for } z \in \mathcal{N} \text{ and } T \in \mathcal{T}(z)$$

and

$$g^\star|_{E \cap \partial\omega_z^\star} := d \int_E g \varphi_z \, dx / |E| \quad \text{for } z \in \mathcal{N} \text{ and } E \in \mathcal{E}(z) \cap \mathcal{E}_N.$$

An approximation of the integral in G is given by

$$\gamma^\star|_{T \cap \omega_z^\star} := (d+1) \delta_T \int_T \widehat{f} \beta \cdot \nabla \varphi_z \, dx / |T| \quad \text{for } z \in \mathcal{N} \text{ and } T \in \mathcal{T}(z).$$

Locally, the Luce-Wohlmuth equilibrator reads

$$\widehat{q}_{\mathrm{LW}}|_{\omega_z^\star} := \operatorname*{argmin}_{\tau_h \in Q(\mathcal{T}^\star(z))} \left\| K^{-1/2} (\sigma_h - \tau_h) \right\|_{L^2(\omega_z^\star)}$$

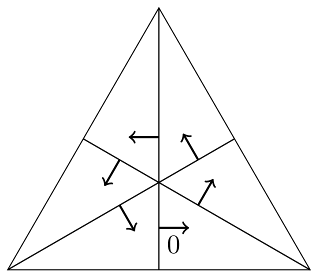

ABBILDUNG 1. Schematic view of the divergence correction $\tau \in \mathrm{RT}_0(\mathcal{T}^\star(T))$ on some element $T \in \mathcal{T}$.

with

$$Q(\mathcal{T}^\star(z)) := \big\{\tau_h \in \mathrm{RT}_0(\mathcal{T}^\star(z)) \mid f^\star + \operatorname{div}\tau_h + \gamma^* = 0 \text{ in } \omega_z^\star,\\ g^\star - \tau_h \cdot \nu = 0 \text{ along } \partial\omega_z^\star \cap \Gamma_N \;\&\; \tau_h \cdot \nu = \sigma_h \cdot \nu \text{ along } \partial\omega_z^\star \setminus \partial\Omega\big\}.$$

The well-posedness of this minimisation for $z \in \mathcal{N} \setminus \mathcal{N}(\Gamma_D)$ follows from $\mathcal{R}es_{\mathrm{SDM}}(\varphi_z) = 0$ and the complementary condition

$$\int_{\omega_z^*} \operatorname{div} q_{\mathrm{LW}}\, dx = \int_{\omega_z^*} \sigma_h \cdot \nu\, ds = -\int_{\omega_z} \widehat{f}\varphi_z\, dx - \int_{\partial\omega_z \cap \Gamma_N} g\varphi_z\, ds - G(\varphi_z)\\ = -\int_{\omega_z^\star} (f^\star + \gamma^\star)\, dx - \int_{\partial\omega_z \cap \Gamma_N} g^\star\, ds.$$

By continuity of σ_h along $\partial\omega_z^\star$, this well defines $q_{\mathrm{LW}} \in H(\operatorname{div}, \Omega)$ with $\operatorname{div} q_{\mathrm{LW}} + f^\star + \gamma^\star = 0$ and $q_{\mathrm{LW}} \cdot \nu - g^\star = 0$ along Γ_N.

To determine a Raviart-Thomas function $q_{\mathrm{LW}} \in \mathrm{RT}_0(\mathcal{T}^\star)$ with $\operatorname{div} q_{\mathrm{LW}} + f^\star \equiv 0$, it is possible to add a (nonunique) correction $\tau \in \mathrm{RT}_0(\mathcal{T}^\star)$ with $\operatorname{div}\tau|_{T^\star} + \gamma^* = 0$ for all $T^\star \in \mathcal{T}^\star(T)$, $\tau|_T \cdot \nu_T = 0$ and $\int_T \operatorname{div}\tau\, dx = 0$ for all $T \in \mathcal{T}$, since $\sum_{z \in \mathcal{N}(T)} \nabla\varphi_z = 0$ and hence

$$\int_T \gamma^*\, dx = (d+1) \sum_{z \in \mathcal{N}(T)} \delta_T \int_T \widehat{f}\beta \cdot \nabla\varphi_z\, dx = 0.$$

The final equilibrator reads $q_{\mathrm{LW}} := \widehat{q}_{\mathrm{LW}} + \tau$ and leads to the error estimator η_{LW} given below.

Remark 3.1. The actual implementation in 2D computes $\tau \in \mathrm{RT}_0(\mathcal{T}^\star(T))$ locally on every $T \in \mathcal{T}$ with $\tau \cdot \nu_T = 0$ along ∂T by a clockwise algorithm as illustrated in Figure 1. The choice of the interior fluxes is unique up to an additional constant which, for simplicity, is chosen such that $\tau \cdot \nu_E = 0$ on the first face. Certainly, this is not optimal and leaves room for further improvement.

Theorem 3.1 with $\widehat{f}_h = f^\star$ and $g_h = g^\star$ yields the error estimator

$$\|\!|\mathcal{R}es|\!\|_* \le \left(\sum_{T \in \mathcal{T}} \left(\eta_{R,T}(q_{\mathrm{LW}}) + \eta_{\mathrm{DF},T}(q_{\mathrm{LW}})\right)^2\right)^{1/2} =: \eta_{\mathrm{LW}}.$$

3.2.3. *Global minimisation.* A global minimisation computes

$$q_{\mathrm{MFEM}} = \operatorname*{argmin}_{\substack{q \in \mathrm{RT}_0(\mathcal{T})\\ \operatorname{div} q + \widehat{f}_h = 0\\ q\cdot\nu - g_h = 0 \text{ along } \Gamma_N}} \left\| K^{-1/2}(\sigma_h - q) \right\|_{L^2(\Omega)}$$

for the piecewise integral mean $\widehat{f}_h = \widehat{f}_{\mathcal{T}}$ of f and the facewise integral mean $g_h = g_{\mathcal{E}_N}$ of g.

Theorem 3.1 leads to the error estimator

$$\|\!|\mathcal{R}es|\!\|_* \le \left(\sum_{T \in \mathcal{T}} \left(\eta_{R,T}(q_{\mathrm{MFEM}}) + \eta_{\mathrm{DF},T}(q_{\mathrm{MFEM}})\right)^2\right)^{1/2} =: \eta_{\mathrm{MFEM}}.$$

The nomenclature of this estimator stems from the fact that q_{MFEM} is also the Raviart-Thomas mixed FEM solution of the problem

$$-\operatorname{div}(K\nabla w) = \widehat{f} \text{ in } \Omega,\ w = u_h \text{ along } \Gamma_D \text{ and } K\nabla w \cdot \nu = g \text{ along } \Gamma_N.$$

3.2.4. *Postprocessing of the numerical flux in 2D.* The postprocessing from [CM12a] leads to improved efficiency of the error estimator. The main idea of this postprocessing is to replace q by $q + \operatorname{Curl} v$ for some discrete function $v \in H^1(\Omega)$ such that $\left\|K^{-1/2}(\sigma_h - q - \operatorname{Curl} v)\right\| \leq \left\|K^{-1/2}(\sigma_h - q)\right\|$. This is done by some preconditioned CG (PCG) scheme with initial value zero for the minimiser of

$$\underset{\substack{v\in P_1(\widehat{\mathcal{T}})\cap C(\Omega)\\ \operatorname{Curl} v\cdot\nu=0 \text{ along } \Gamma_N}}{\operatorname{argmin}} \left\|K^{-1/2}(\sigma_h - q - \operatorname{Curl} v)\right\| \tag{3.8}$$

on some triangulation $\widehat{\mathcal{T}}$. Since on $\widehat{\mathcal{T}} = \mathcal{T}$ and for $q = q_{\mathrm{MFEM}}$ an improvement of q is only possible if v is designed in a larger approximation space than $P_1(\mathcal{T}) \cap C(\Omega)$, see [CM12a]. For η_{B}, this is performed with $j = 1$ or $j = 2$ red refinements $\widehat{\mathcal{T}} := \operatorname{red}^j(\mathcal{T})$ of $\mathcal{T}$. For the Luce-Wohlmuth equilibrator error estimator, we employ $\widehat{\mathcal{T}} := \mathcal{T}^\star$. The number of red-refinements and the number of PCG iterations is denoted in the label of the postprocessed error estimators. For instance, $\eta_{\mathrm{Br}(1)}$ employs $\widehat{\mathcal{T}} := \operatorname{red}(\mathcal{T})$ and performs one PCG iteration, $\eta_{\mathrm{Brr}(3)}$ employs $\widehat{\mathcal{T}} := \operatorname{red}^2(\mathcal{T})$ and performs three PCG iteration and $\eta_{\mathrm{LW}(\infty)}$ employs $\widehat{\mathcal{T}} := \mathcal{T}^\star$ and computes the optimal $v \in P_1(\mathcal{T}^\star) \cap C(\Omega)$ in (3.8).

A second postprocessing step improves the divergence of the equilibrator q. After every red-refinement the three new interior fluxes in any triangle are modified such that $\operatorname{div} q + \widehat{f}_{\mathrm{red}(\mathcal{T})} = 0$ for the piecewise integral mean $\widehat{f}_{\mathrm{red}(\mathcal{T})}$ of f with respect to the red-refined triangulation. Since the normal fluxes on the old faces of $\mathcal{T}$ remain unchanged, this is a very cheap step that reduces the oscillation contribution $\eta_{R,T}(q)$. If this step is performed, another "m" is included in the label, e.g. $\eta_{\mathrm{Bmrr}(3)}$ instead of $\eta_{\mathrm{Brr}(3)}$.

A similar strategy in 3D is possible but one has to replace the red-refinement by a proper 3D refinement and the ansatz functions for the postprocessing have now three components, i.e., $v \in H^1(\Omega)^3$.

3.3. **Inhomogeneous Dirichlet boundary conditions.** This subsection employs the construction from [BCD04] to allow guaranteed upper error bounds also in presence of inhomogeneous Dirichlet boundary data u_D.

Theorem 3.2. *For $u_D \in H^1(\Gamma_D) \cap H^2(\mathcal{E}(\Gamma_D))$ there exists $w_D \in H^1(\Omega)$ with $w_D = u - u_D$ along Γ_D. Then*

$$|||u - u_h|||^2 \leq |||\mathcal{R}es|||_*^2 + |||w_D|||^2$$

where

$$|||w_D|||^2 \leq \sum_{E\in\mathcal{E}(\Gamma_D)} m_{E,D}^2 \left\|\partial^2 u_D/\partial s^2\right\|_{L^2(E)}^2$$

with

$$m_{E,D} := C_{D,1}(E) h_E^{3/2} \lambda_{\max}(K,T)^{1/2} + C_{D,2}(E) h_E^{5/2} \left\|\mu - \operatorname{div}\beta/2\right\|_{L^\infty(E)}^{1/2}.$$

Beweis. Let w denote the solution of the problem

$$-\nabla(K\nabla w) + \beta\cdot\nabla w + \mu w = 0 \qquad \text{in } \Omega,$$

$$w = u - u_D \quad \text{on } \Gamma_D \qquad \text{and} \qquad K\frac{\partial w}{\partial n} = 0 \quad \text{on } \Gamma_N.$$

The orthogonality $a(w, v) = 0$ for all $v \in V$ leads to the Pythagoras theorem

$$|||u - u_h|||^2 = |||u - u_h - w|||^2 + |||w|||^2.$$

It remains to show $|||u - u_h - w||| \leq |||\mathcal{R}es|||_*$ which follows from testing $\mathcal{R}es(v)$ with the admissible test function $v = u - u_h - w$.

Any other $w_D \in H^1(\Omega)$ with $w_D = u - u_D$ along Γ_D leads to $w - w_D \in V$ and, again with $a(w, w - w_D) = 0$, this yields

$$|||w_D|||^2 = |||w_D - w|||^2 + |||w|||^2 \geq |||w|||^2.$$

The design from [BCD04] leads to such a w_D that allows the asserted estimate. $\square$

Remark 3.2. In 2D, the constant $C_{D,1}(E)$ in (3.2) was calculated in [CM13]. The constant $C_{D,2}(E)$ in (3.2) can be estimated in a similar fashion, see [Mer13] for details. For triangulations into right isosceles triangles, the constants are bounded by $C_{D,1} \leq 0.4980$ and $C_{D,2} \leq 0.0654$.

4. Efficiency

This sections deals with the efficiency of the derived error estimators with respect to an augmented norm due to [Ver05] in the convection-dominated case.

4.1. **Augmented norm estimates.** In [Ver05] the dual norm of some convection dependent term was added to the energy error norm to allow for robust error estimates. A similar approach was employed in the context of discontinuous Galerkin methods in [ESV10] where this norm was coined augmented norm, also see [AABR13]. The following ideas are based on the same technique. However, since we use a classic conforming FEM, the formulations of the augmented norm and of the error estimators simplify somewhat.

We introduce the augmented energy norm for all $v \in V$ defined by

$$\left\lVert\!\left\lvert v \right\rvert\!\right\rVert_{\oplus} := \left\lVert\!\left\lvert v \right\rvert\!\right\rVert + \sup_{\substack{\varphi \in V \\ \left\lVert\!\left\lvert \varphi \right\rvert\!\right\rVert = 1}} a_A(v, \varphi). \tag{4.1}$$

Theorem 4.1. *With the discrete approximation $u_h \in V_h$ and the error estimator of Theorem 3.1, it holds*

$$\left\lVert\!\left\lvert u - u_h \right\rvert\!\right\rVert_{\oplus} \leq 3\eta. \tag{4.2}$$

Beweis. With the splitting (2.2) we deduce

$$\begin{aligned} \left\lVert\!\left\lvert u - u_h \right\rvert\!\right\rVert_{\oplus} &= \left\lVert\!\left\lvert u - u_h \right\rvert\!\right\rVert + \sup_{\substack{v \in V \\ \left\lVert\!\left\lvert v \right\rvert\!\right\rVert = 1}} a_A(u - u_h, v) && (4.3) \\ &= \left\lVert\!\left\lvert u - u_h \right\rvert\!\right\rVert + \sup_{\substack{v \in V \\ \left\lVert\!\left\lvert v \right\rvert\!\right\rVert = 1}} \left(a(u - u_h, v) - a_S(u - u_h, v) \right). && (4.4) \end{aligned}$$

The second term in the supremum can be bounded by

$$\begin{aligned} a_S(u - u_h, v) &= \int_\Omega K \nabla (u - u_h) \cdot \nabla v \, dx + \int_\Omega (\mu - \frac{1}{2} \operatorname{div} \beta)(u - u_h) v \, dx \\ &\leq \left\lVert\!\left\lvert u - u_h \right\rvert\!\right\rVert \left\lVert\!\left\lvert v \right\rvert\!\right\rVert. \end{aligned}$$

This yields

$$\sup_{\substack{v \in V \\ \left\lVert\!\left\lvert v \right\rvert\!\right\rVert = 1}} a_S(u - u_h, v) \leq \left\lVert\!\left\lvert u - u_h \right\rvert\!\right\rVert.$$

It thus follows

$$\left\lVert\!\left\lvert u - u_h \right\rvert\!\right\rVert_{\oplus} \leq 2 \left\lVert\!\left\lvert u - u_h \right\rvert\!\right\rVert + \sup_{\substack{v \in V \\ \left\lVert\!\left\lvert v \right\rvert\!\right\rVert = 1}} a(u - u_h, v)$$

which completes the proof. $\square$

Remark 4.1. It was recently shown in [JN13] that, under certain hypotheses, some residual estimator is robust in the induced energy norm of the SDM stabilised FEM.

4.2. **Equivalence to standard residual-based error estimators.** All equilibration designs above are known to be efficient in the sense

$$\eta_{\mathrm{DF},T}(q)^2 \lesssim h_T^2 c_{K,T}^{-1} \left\lVert \widehat{f} \right\rVert_{L^2(T)}^2 + \sum_{E \in \mathcal{E}(T)} h_E c_{K,\omega_E}^{-1} \left\lVert [\sigma_h \cdot \nu_E]_E \right\rVert_{L^2(E)}^2, \tag{4.5}$$

see e.g. [AABR13, BS08] for (an upper bound of) η_B, or [LW04] for η_{LW} or [CFPV09] for a similar result also in 3D. For completeness, the efficiency for η_B is proven below.

Theorem 4.2 (Efficiency of η_B)**.** *For the equilibrated quantity $q = q_B$ from Section 3.2.1, it holds*

$$\eta_{\mathrm{DF},T}(q)^2 \lesssim h_T^2 c_{K,T}^{-1} \left\|\widehat{f}\right\|_{L^2(T)}^2 + \sum_{E\in\mathcal{E}(T)} h_E c_{K,\omega_E}^{-1} \left\|[\sigma_h \cdot \nu_E]_E\right\|_{L^2(E)}^2 .$$

Beweis. The remainder $r := q_B - \sigma_h = \sum_{z\in\mathcal{N}} q_z \in RT_{-1}(\mathcal{T}(z))$ satisfies $\eta_{\mathrm{DF},T}(q) = \left\|K^{-1/2} r\right\|_{L^2(T)}$, $\operatorname{div} r = -\widehat{f}_T$, $[r\cdot\nu_E] = -[\sigma_h \cdot \nu_E]$ on all interior faces $E \in \mathcal{E}$, and $r\cdot\nu_E = g_{\mathcal{E}_n} - \sigma_h\cdot\nu_E$ on $E \in \mathcal{E}_N$.

The constraints for the design of q_B from Section 3.2.1 and the reference [BS08, Lemma 3] (for $g_T = \widehat{f}_z|_T$ and $g_F = -1/d[\sigma_h\cdot\nu_F]$ or $g_F = g_z - 1/d\sigma_h\cdot\nu_F$ for $F\in\mathcal{E}_N$) show

$$\left\|K^{-1/2} q_z\right\|_{L^2(T)} \lesssim \sum_{T\in\mathcal{T}(z)} h_T \left\|\widehat{f}_z|_T\right\|_{L^2(T)} + \sum_{E\in\mathcal{E}(z)} h_T^{1/2} \left\|[\sigma_h\cdot\nu_E]\right\|_{L^2(E)} .$$

Elementary calculations show

$$\left\|\widehat{f}_z|_T\right\|_{L^2(T)} \lesssim \left\|\widehat{f}\right\|_{L^2(T)}^2 \quad \text{for all } T\in\mathcal{T},$$
$$\left\|g_z|_E - 1/d\,\sigma_h\cdot\nu_E\right\|_{L^2(E)} \lesssim \left\|g - \sigma_h\cdot\nu\right\|_{L^2(E)}^2 \quad \text{for all } E\in\mathcal{E}_N.$$

Here, the additional terms due to the stabilisation are hidden by the estimate

$$\left\|\frac{\delta_T}{|T|}\int_T \widehat{f}\beta\cdot\nabla\varphi_z\right\|_{L^2(T)}^2 = \frac{\delta_T^2}{|T|}\left(\int_T \widehat{f}\beta\cdot\nabla\varphi_z\right)^2 \lesssim \left\|\widehat{f}\right\|_{L^2(T)}^2 .$$

Together with a triangle inequality, this results in

$$\begin{aligned}\left\|K^{-1/2} r\right\|_{L^2(T)} &\le \sum_{z\in\mathcal{N}(T)} \left\|K^{-1/2} q_z\right\|_{L^2(T)}\\ &\lesssim \sum_{z\in\mathcal{N}(T)} c_{K,\omega_T}^{-1}\Big(\sum_{T\in\mathcal{T}(z)} h_T\left\|\widehat{f}\right\|_{L^2(T)} + \sum_{E\in\mathcal{E}(z)} h_E^{1/2}\left\|[\sigma_h\cdot\nu_E]\right\|_{L^2(E)}\Big).\end{aligned}$$

Further considerations involving finite overlap constants and local eigenvalue quotients, e.g. $c_{K,T}$ vs. c_{K,ω_T}, conclude the proof.

□

The terms on the right-hand side of (4.5) are in fact the contributions of a residual-based error estimator as in [Ver05] for the convection-dominated case $\mu = 0$. In this reference, this estimator was shown to exhibit robust efficiency only with respect to the augmented norm $|||u - u_h|||_{\oplus}$. Thus, the equilibration error estimators in the present designs are also efficient independently of the coefficients in the augmented norm $|||u - u_h|||_{\oplus}$ due to equivalence with the residual error estimator. However, this cannot be expected for the efficiency with respect to the energy norm $|||u - u_h|||$. Moreover, in the reaction dominated case, $\eta_{\mathrm{DF},T}(q)$ is, in this form, not robust with respect to $|||u - u_h|||$ in the preasymptotic range. The problems arise from the suboptimal estimate

$$\int_\Omega K^{-1/2}(q-\sigma_h)\cdot K^{1/2}\nabla v\,dx \le \left\|K^{-1/2}(q-\sigma_h)\right\|_{L^2(\Omega)} |||v|||$$

in the proof of Theorem 3.1. However, [CFPV09] shows a possible remedy for these difficulties.

5. Numerical Experiments

In this section, we present several numerical examples which illustrate the performance of the a posteriori error estimators of Section 3. Three convection dominated problems and one singularly perturbed problem are used as benchmarks. The numerical solution of (1.1) on the unit square $\Omega = (0,1)^2$ is obtained with conforming first order FEM and SDM. All examples exhibit typical boundary layers and possibly large initial oscillations which are both resolved by the adaptive algorithm. The chosen test cases can also be found in [Joh00, PV00, ESV10, Ste05] and enable a comparison of the results.

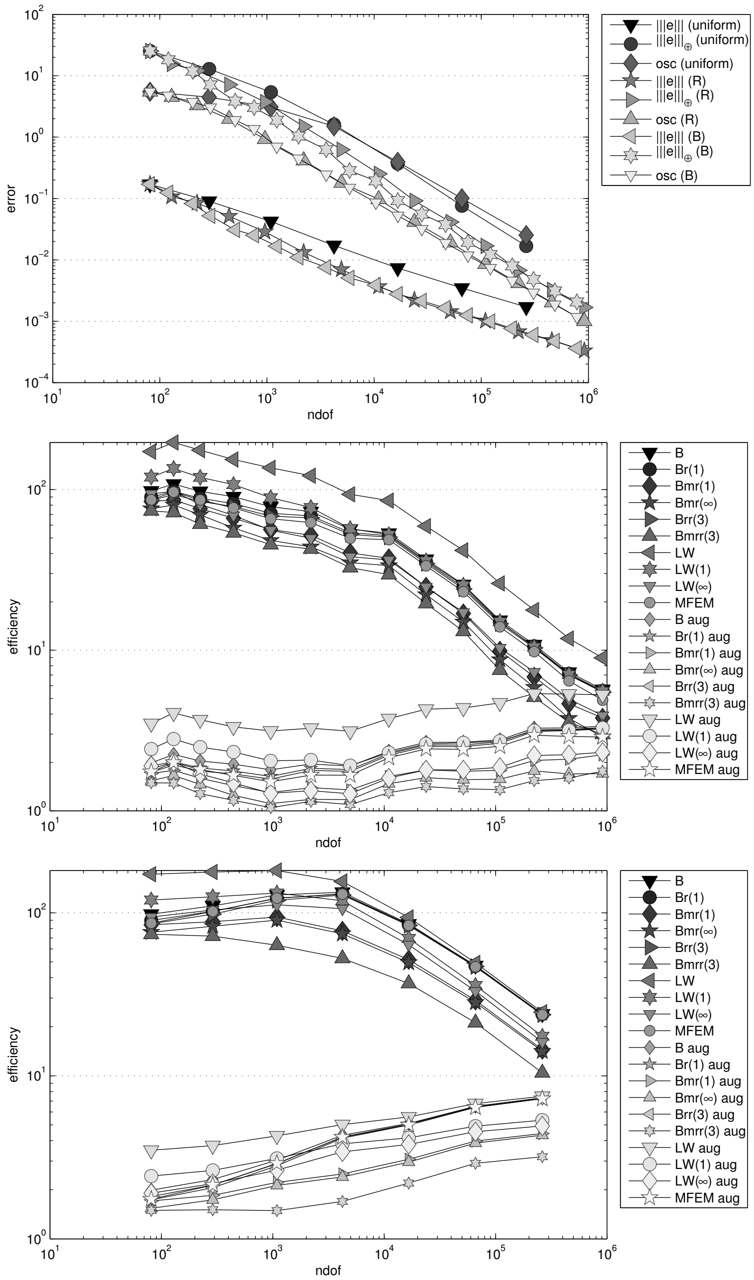

ABBILDUNG 2. Example 1 with $K = 10^{-4} I_2$. Error in energy norm, augmented norm and oscillations for uniform and adaptive refinement versus number of degrees of freedom [top]. Efficiency indices of different error estimators with regard to energy norm and augmented norm (labelled with aug) for adaptively refined meshes after η_R [center]. Efficiency indices of different error estimators with regard to energy norm and augmented norm for uniformly refined meshes [bottom]. Error estimators η_{xyz} are labelled xyz.

The bulk marking algorithm (also known as Dörfler or greedy marking) based on the element-wise refinement indicator η_R [Ver05] is employed in all experiments to avoid a biased refinement. It is defined on each $T \in \mathcal{T}$ for the exact solution $u \in V$ and the numerical approximation $u_h \in V_h$ by

$$\eta_R^2(T) := \alpha_T^2 \left\| \widehat{f} \right\|_{L^2(T)}^2 + \sum_{E \in \mathcal{E}(T)} \alpha_{T,E} \left\| [K \nabla u_h \cdot \nu_E]_E \right\|_{L^2(E)}^2$$

with

$$\alpha_T := \min\{h_T K^{-1/2}, 1\} \qquad \text{and} \qquad \alpha_{T,E} := K^{-1/2} \min\{h_E K^{-1/2}, 1\}.$$

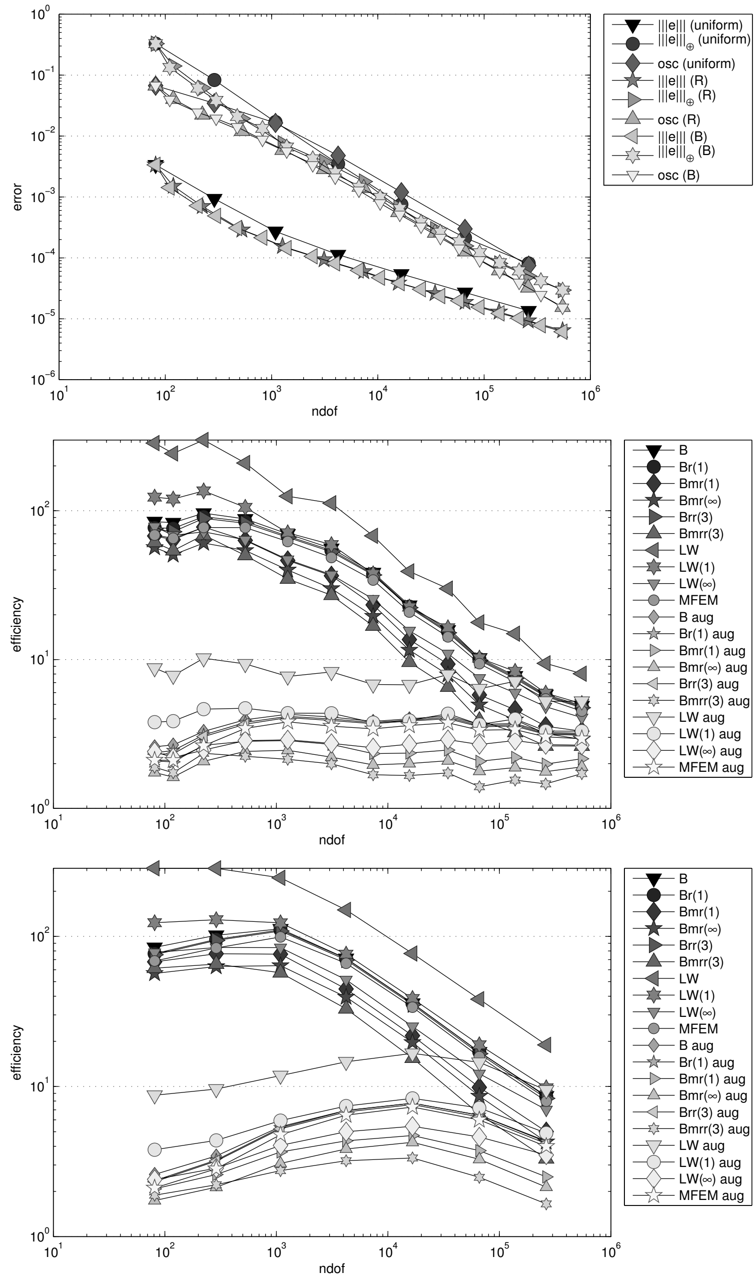

ABBILDUNG 3. Example 2 with $K = 10^{-4} I_2$. Error in energy norm, augmented norm and oscillations for uniform and adaptive refinement versus number of degrees of freedom [top]. Efficiency indices of different error estimators with regard to energy norm and augmented norm (labelled with aug) for adaptively refined meshes after η_R [center]. Efficiency indices of different error estimators with regard to energy norm and augmented norm for uniformly refined meshes [bottom]. Error estimators η_{xyz} are labelled xyz.

Alternatively, a local version of the equilibration estimator η_B is used. Then, $\eta_B^2(T) := \eta_{R,T}(q_B)^2 + \eta_{\mathrm{DF},T}(q_B)^2$ replaces $\eta_R^2(T)$. Naturally, any other error equilbration estimator yields refinement indicators in the same fashion. For some bulk parameter $0 < \Theta \leq 1$, the refinement algorithm finds the smallest set of elements $\mathcal{M} \subset \mathcal{T}$ such that

$$\Theta \sum_{T \in \mathcal{T}} \eta(T) \leq \sum_{T \in \mathcal{M}} \eta(T).$$

To determine $\mathcal{M}$, all refinement indicators $\eta(T)$ are sorted in descending order. Then, elements are added to the refinement set, starting from the largest error contribution, until the inequality is valid. The resulting $\mathcal{M}$ is the smallest set of elements for refinement. Different marking strategies are possible and can lead to differently adapted meshes, see [PV00] for a study of several algorithms. The mesh is refined at least for the elements in τ with possible additional refinements to re-establish conformity of the mesh. For the numerical results in this section, we employ $\Theta = 0.5$.

The efficiency indices for some error estimator η are computed by the quotient $\eta / \|\!|e|\!\|$ or $\eta / \|\!|e|\!\|_{\oplus}$, respectively.

Example 1. We consider (1.1) for the scalar diffusion value $K = 10^{-4} I_2$, $\beta = (2,3)^T$ and $\mu = 2$. The right-hand-side is chosen such that the solution reads

$$u(x,y) = 16x(1-x)y(1-y) \times \left(\frac{1}{2} + \operatorname{atan}\left(\frac{2}{\sqrt{A}} \left(\frac{1}{16} - \left(x - \frac{1}{2}\right)^2 - \left(y - \frac{1}{2}\right)^2 \right) \right) / \pi \right).$$

In this and example 2, we employ some upper bound of the augmented norm (4.1) suggested in [ESV10]. Since β is constant, it holds, for all $v, w \in V$,

$$a_A(v,w) = \int_\Omega (\beta \cdot \nabla v + \frac{1}{2} \operatorname{div} \beta v) w \, dx \le K^{-1/2} \|v\|_{L^2(\Omega)}$$

and thus

$$\|\!|v|\!\|_{\oplus} \le \|\!|v|\!\| + c_{K,\Omega}^{-1/2} \|\beta\|_{L^\infty(\Omega)} \|v\|_{L^2(\Omega)} .$$

Note that since this represents an upper bound of the norm, the error estimators could actually become smaller than this approximation in certain cases, i.e., efficiency indices smaller than 1 could occur in principle.

We observe in Figure 2[top] that the oscillations are quite large and their decay rate is the same as for the augmented norm of the error $\|\!|e|\!\|_{\oplus}$. Hence, the oscillations are not of higher order. Asymptotically, the augmented norm $\|\!|e|\!\|_{\oplus}$ converges to the energy norm $\|\!|e|\!\|$. This is due to the faster convergence of $\|v\|_{L^2(\Omega)}$. We observe that adaptive refinement is clearly superior to uniform refinement and leads to optimal convergence rates. The refinement indicators after η_B result in a qualitatively similar error decay as refinement with η_R. This supports the observations from former experiments for Poisson problems in [CM10] that η_R provides cheap and sufficient refinement indicators for adaptive mesh generation. However, guaranteed bounds are usually not available or overly pessimistic. This justifies the computationally more involved estimators presented here. For the augmented norm, the efficiency indices in Figure 2[center] are constantly at a very good level between 1.5 and 3.5. They differ only marginally for the error estimators B, LW and MFEM and their postprocessings. Due to the high oscillations, the divergence correction significantly reduces the overestimation by a factor $1/5$ even on the finest mesh. The efficiency indices then are in the range 1.3-2.2. In the energy norm, the efficiency indices commence with typically large values at about 100 which decrease monotonically with refinement.

The error estimators show large differences. LW exhibits the largest overestimation which is improved by Braess and MFEM and the best results are achieved for Braess with postprocessing and divergence correction. For uniform mesh refinement, the efficiency indices depicted in Figure 2[bottom] are worse overall and their decay is slower.

Remark 5.1*.* Opposite to the experience with unstabilised first-order FEM for elliptic problems, in this and the following experiments the more involved design of Luce and Wohlmuth is in fact inferior to the approach of Braess possibly due to the modifications required to cope with the stabilisation terms (see Remark 3.1). The postprocessing for the latter seems to remedy this effect but the single PCG iteration in $\eta_{\mathrm{LW}(1)}$ seems not to be sufficient. We thus recommend to use the simpler design of Braess for the discussed problem setting.

Example 2. We consider problem (1.1) with diffusion $K = 10^{-4} I_2,\ \beta = (1,0)^T$ and $\mu = 1$. The right-hand side is chosen such that the solution is given by

$$u(x,y) = \frac{1}{2} x(1-x)y(y-1)(1-\tanh(10-20x)).$$

The comments for experiment 1 in the previous section also hold for the results pictured in Figure 3. We observe the same order for the tested error estimators with efficiency indices in the range 1.3-4 in Figure 3[center]. Again, the large oscillations substantially contribute to the error in the augmented norm as seen in Figure 3[top]. Since they

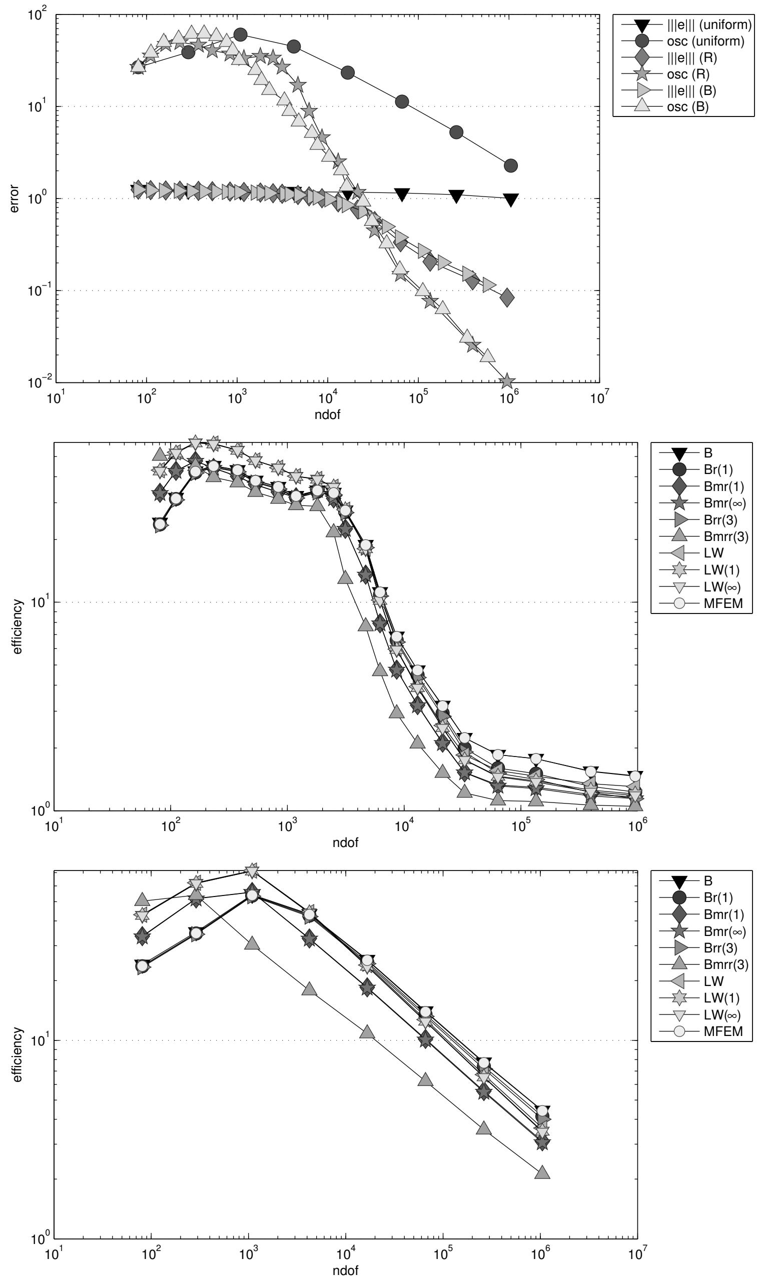

ABBILDUNG 4. Example 3 with $K = 10^{-4} I_2$. Error in energy norm and oscillations for uniform and adaptive refinement versus number of degrees of freedom [top]. Efficiency indices of different error estimators with regard to energy norm for adaptively refined meshes after η_R [center]. Efficiency indices of different error estimators with regard to energy norm for uniformly refined meshes [bottom]. Error estimators η_{xyz} are labelled xyz.

converge with the same rate as the overall error, they are not of higher order. The best estimation is obtained for the Braess estimator with postprocessing and divergence corrections. Altogether, the advantages of adaptive mesh refinement versus uniform mesh refinement can be observed but are not as pronounced as in the first example.

Example 3. We consider a singularly perturbed problem similar to [Ste05] with $K = 10^{-4} I_2$, $\beta = (0, 0)^T$ and $\mu = 1$ which results in strong boundary layers. The right-hand side is chosen such that the solution reads

$$u(x, y) = \delta(x)\delta(y) + \sin(\pi x)\sin(\pi y)$$

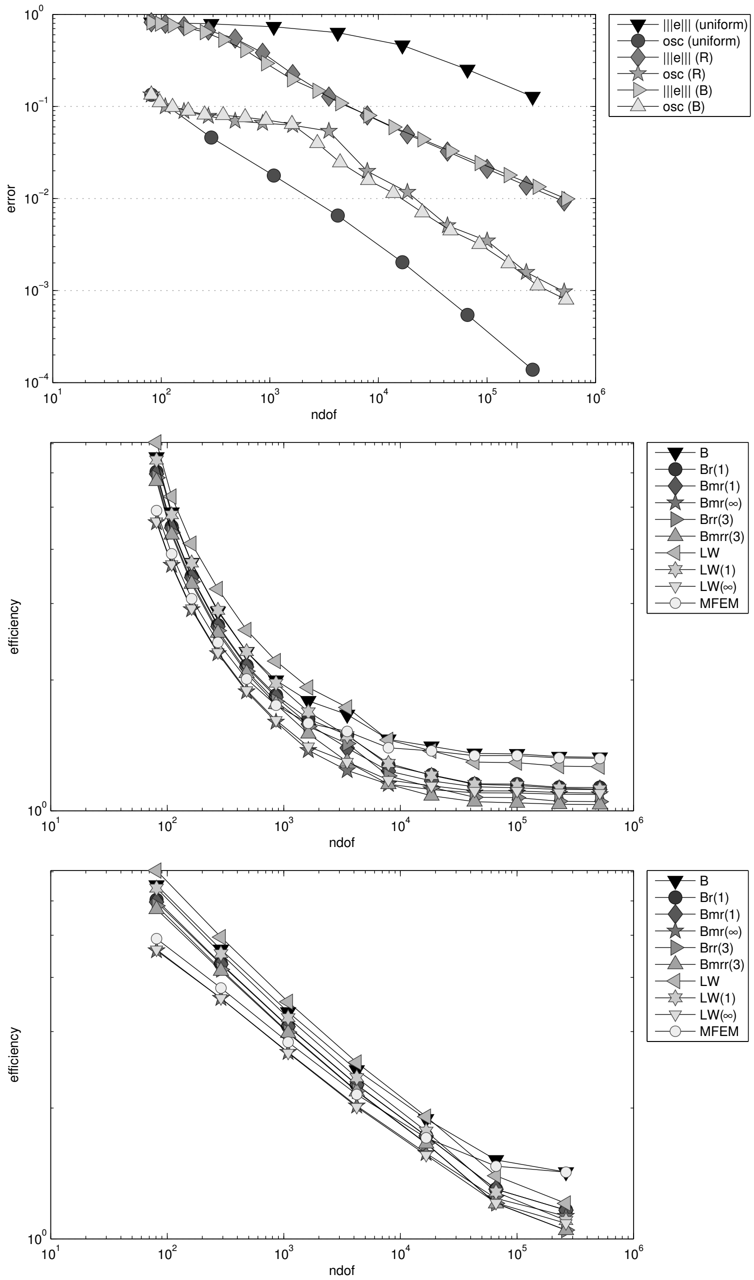

ABBILDUNG 5. Example 4 with $K = 10^{-2} I_2$. Error in energy norm and oscillations for uniform and adaptive refinement versus number of degrees of freedom [top]. Efficiency indices of different error estimators with regard to energy norm for adaptively refined meshes after η_R [center]. Efficiency indices of different error estimators with regard to energy norm for uniformly refined meshes [bottom]. Error estimators η_{xyz} are labelled xyz.

where

$$\delta(z) := 1 - \frac{\alpha(z) + \alpha(1-z)}{1 + \alpha(1)} \quad \text{and} \quad \alpha(z) := e^{-\frac{1}{\sqrt{2K}} z}.$$

The solution exhibits very large oscillations. The error does not show any reduction with uniform refinement and the oscillations are reduced with a low rate, see Figure 4[top]. In contrast to that, adaptive refinement with either η_R or η_B performs considerably better with the expected reduction rate after a pre-asymptotic phase. For a large number of degrees of freedom, the efficiency indices are in the range 1.03-1.7 as illustrated in Figure 4[center]. Due to the large oscillations, the error estimator $\eta_{\mathrm{Bmrr(3)}}$ with the divergence correction leads to substantially better efficiency indices. Thus, the error estimators are nearly exact. This is comparable to the results for the Poisson model problem, see [CM12a]. Although the uniform refinement does not reduce the energy error, the efficiency indices decrease in accordance to the oscillations. The error convergence rates for uniform refinements are identical to the oscillation reduction rate, see Figure 4[bottom].

Example 4. We consider (1.1) for the diffusion $K = 10^{-2} I_2$, $\beta = (2,3)^T$ and $\mu = 1$. The right-hand-side is chosen such that the solution reads

$$u(x, y) = xy^2 - y^2\alpha(2(x-1)) - x\alpha(3(y-1)) + \alpha(2(x-1) + 3(y-1))$$

with

$$\alpha(v) := \exp(v/K).$$

The oscillations in this example are of higher order as depicted in Figure 5[top]. As with the Poisson model problem, asymptotically the error estimators become nearly exact with efficiency indices in the range 1.03-1.7 on meshes with more than 300 degrees of freedom with refinement based on η_R or η_B, see Figure 5[center]. The suggested postprocessing shows a large effect on the efficiency while the divergence correction only has a small influence due to the small oscillations. For uniform mesh refinement there is a long pre-asymptotic phase.

LITERATUR

[AABR13] Mark Ainsworth, Alejandro Allendes, Gabriel R. Barrenechea, and Richard Rankin. Fully computable a posteriori error bounds for stabilised FEM approximations of convection-reaction-diffusion problems in three dimensions. *International Journal for Numerical Methods in Fluids*, 73(9):765–790, 2013.

[BC04] S.C. Brenner and C. Carstensen. *Finite Element Methods*. John Wiley and Sons, 2004.

[BCD04] S. Bartels, C. Carstensen, and G. Dolzmann. Inhomogeneous Dirichlet conditions in a priori and a posteriori finite element error analysis. *Numer. Math.*, 99(1):1–24, 2004.

[Beb03] M. Bebendorf. A note on the Poincaré inequality for convex domains. *Z. Anal. Anwendungen*, 22(4):751–756, 2003.

[BS08] Dietrich Braess and Joachim Schöberl. Equilibrated residual error estimator for edge elements. *Math. Comp.*, 77(262):651–672, 2008.

[CEHL12] Carsten Carstensen, Martin Eigel, Ronald H.W. Hoppe, and Caroline Löbhard. A review of unified a posteriori finite element error control. *Numer. Math. Theor. Meth. Appl.*, 5(4):509–558, 2012.

[CFPV09] Ibrahim Cheddadi, Radek Fučík, Mariana I. Prieto, and Martin Vohralík. Guaranteed and robust a posteriori error estimates for singularly perturbed reaction-diffusion problems. *M2AN Math. Model. Numer. Anal.*, 43(5):867–888, 2009.

[Cia78] Philippe G. Ciarlet. *The finite element method for elliptic problems*. North-Holland Publishing Co., Amsterdam, 1978. Studies in Mathematics and its Applications, Vol. 4.

[CM10] Carsten Carstensen and Christian Merdon. Estimator competition for Poisson problems. *J. Comp. Math.*, 28(3):309–330 (electronic), 2010.

[CM12a] Carsten Carstensen and Christian Merdon. Effective postprocessing for equilibration a posteriori error estimators. *Numer. Math*, 2012.

[CM12b] Carsten Carstensen and Christian Merdon. Refined fully explicit a posteriori residual-based error control (submitted). 2012+.

[CM13] C. Carstensen and C. Merdon. Computational survey on a posteriori error estimators for nonconforming finite element methods for the Poisson problem. *J. Comput. Appl. Math.*, 249:74–94, 2013.

[DM99] Philippe Destuynder and Brigitte Métivet. Explicit error bounds in a conforming finite element method. *Math. Comp.*, 68(228):1379–1396, 1999.

[EJ93] Kenneth Eriksson and Claes Johnson. Adaptive streamline diffusion finite element methods for stationary convection-diffusion problems. *Math. Comp.*, 60(201):167–188, S1–S2, 1993.

[ESV10] Alexandre Ern, Annette F. Stephansen, and Martin Vohralík. Guaranteed and robust discontinuous Galerkin a posteriori error estimates for convection-diffusion-reaction problems. *J. Comput. Appl. Math.*, 234(1):114–130, 2010.

[HB79] T. J. R. Hughes and A. Brooks. A multidimensional upwind scheme with no crosswind diffusion. In *Finite element methods for convection dominated flows (Papers, Winter Ann. Meeting Amer. Soc. Mech. Engrs., New York, 1979)*, volume 34 of *AMD*, pages 19–35. Amer. Soc. Mech. Engrs. (ASME), New York, 1979.

[HMM86] Thomas J. R. Hughes, Michel Mallet, and Akira Mizukami. A new finite element formulation for computational fluid dynamics. II. Beyond SUPG. *Comput. Methods Appl. Mech. Engrg.*, 54(3):341–355, 1986.

[JN13] Volker John and Julia Novo. A robust SUPG norm a posteriori error estimator for stationary convectionâĂŞdiffusion equations. *Math. Comput. Simulation*, 255(1):289–305, 2013.

[JNP84] Claes Johnson, Uno Nävert, and Juhani Pitkäranta. Finite element methods for linear hyperbolic problems. *Comput. Methods Appl. Mech. Engrg.*, 45(1-3):285–312, 1984.

[Joh90] Claes Johnson. Adaptive finite element methods for diffusion and convection problems. *Comput. Methods Appl. Mech. Engrg.*, 82(1-3):301–322, 1990. Reliability in computational mechanics (Austin, TX, 1989).

[Joh00] Volker John. A numerical study of a posteriori error estimators for convection-diffusion equations. *Comput. Methods Appl. Mech. Engrg.*, 190(5-7):757–781, 2000.

[LS10] R. S. Laugesen and B. A. Siudeja. Minimizing Neumann fundamental tones of triangles: an optimal Poincaré inequality. *J. Differential Equations*, 249(1):118–135, 2010.

[LW04] R. Luce and B. I. Wohlmuth. A local a posteriori error estimator based on equilibrated fluxes. *SIAM J. Numer. Anal.*, 42(4):1394–1414 (electronic), 2004.

[Mer13] C. Merdon. *Aspects of guaranteed error control in computation for partial differential equations*. PhD thesis, 2013.

[PV00] Areti Papastavrou and Rüdiger Verfürth. A posteriori error estimators for stationary convection-diffusion problems: a computational comparison. *Comput. Methods Appl. Mech. Engrg.*, 189(2):449–462, 2000.

[PW60] L. E. Payne and H. F. Weinberger. An optimal Poincaré inequality for convex domains. *Arch. Rat. Mech. Anal.*, 5:286–292, 1960.

[Rep08] Sergey Repin. *A posteriori estimates for partial differential equations*, volume 4 of *Radon Series on Computational and Applied Mathematics*. Walter de Gruyter GmbH & Co. KG, Berlin, 2008.

[RS06] Sergey Repin and Stefan Sauter. Functional a posteriori estimates for the reaction-diffusion problem. *C. R. Math. Acad. Sci. Paris*, 343(5):349–354, 2006.

[Ste05] Rob Stevenson. The uniform saturation property for a singularly perturbed reaction-diffusion equation. *Numer. Math.*, (101):355–379 (electronic), 2005.

[Ver98] Rüdiger Verfürth. A posteriori error estimators for convection-diffusion equations. *Numer. Math.*, 80(4):641–663, 1998.

[Ver05] Rüdiger Verfürth. Robust a posteriori error estimates for stationary convection-diffusion equations. *SIAM J. Numer. Anal.*, 43(4):1766–1782 (electronic), 2005.

[Voh07] Martin Vohralík. A posteriori error estimates for lowest-order mixed finite element discretizations of convection-diffusion-reaction equations. *SIAM J. Numer. Anal.*, 45(4):1570–1599 (electronic), 2007.